

# Supramolecular Polymerization from Polypeptide-Grafted Comb Polymers

Jing Wang,<sup>†</sup> Hua Lu,<sup>‡</sup> Ranjan Kamat,<sup>†</sup> Sai V. Pingali,<sup>§</sup> Volker S. Urban,<sup>§</sup> Jianjun Cheng,<sup>\*,†</sup> and Yao Lin<sup>\*,†,||</sup>

<sup>†</sup>Polymer Program, Institute of Materials Science and <sup>||</sup>Department of Chemistry, University of Connecticut, Storrs, Connecticut 06269, United States

<sup>‡</sup>Department of Materials Science and Engineering, University of Illinois at Urbana-Champaign, Urbana, Illinois 61801, United States

<sup>§</sup>Center for Structural Molecular Biology, Neutron Scattering Science Division, Oak Ridge National Laboratory, Oak Ridge, Tennessee 37831, United States

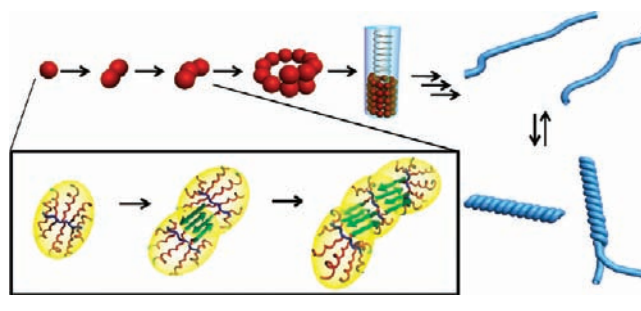
 Supporting Information

**ABSTRACT:** The helical and tubular structures self-assembled from proteins have inspired scientists to design synthetic building blocks that can be “polymerized” into supramolecular polymers through coordinated noncovalent interactions. However, cooperative supramolecular polymerization from large, synthetic macromolecules remains a challenge because of the difficulty of controlling the structure and interactions of macromolecular monomers. Herein we report the synthesis of polypeptide-grafted comb polymers and the use of their tunable secondary interactions in solution to achieve controlled supramolecular polymerization. The resulting tubular supramolecular structures, with external diameters of hundreds of nanometers and lengths of tens of micrometers, are stable and resemble to some extent biological superstructures assembled from proteins. This study shows that highly specific intermolecular interactions between macromolecular monomers can enable the cooperative growth of supramolecular polymers. The general applicability of this strategy was demonstrated by carrying out supramolecular polymerization from gold nanoparticles grafted with the same polypeptides on the surface.

Global proteins can form helical and tubular superstructures through multiple coordinated interactions (i.e., cooperative supramolecular polymerization), as exemplified by the formation of actin filaments and microtubules.<sup>1</sup> Numerous efforts have been devoted to the design of synthetic building blocks that can mimic such cooperative supramolecular polymerization and be used for controlling the formation of complex, hierarchical structures.<sup>2</sup> While much progress has been made in assembling small molecules to form supramolecular polymers via multiple noncovalent interactions,<sup>3</sup> success has been limited in attempts to use large synthetic polymers as such building blocks.<sup>4</sup> It is still unclear how to accomplish the rational design of macromolecular building blocks that are subject to controlled supramolecular polymerizations.

In order to understand cooperative supramolecular polymerization of macromolecules and eventually use this process to produce well-ordered helical/tubular superstructures, the macromolecular monomers should have well-defined molecular architectures, and the supramolecular polymerization must be controllable and reproducible. We believe that two basic design requirements

**Scheme 1. Schematic Illustration of Supramolecular Polymerization of Polypeptide-Grafted Comb Polymers into Tubular Superstructures**

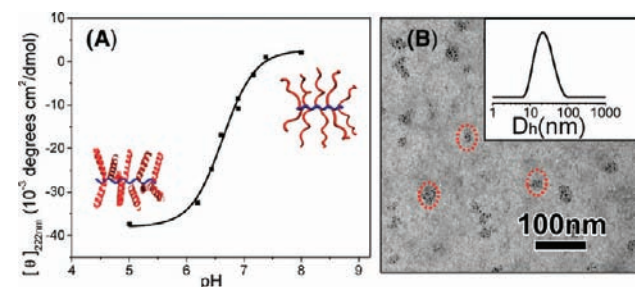
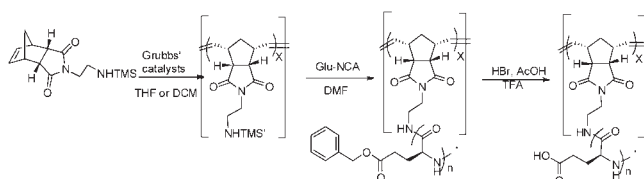


should be met in order to facilitate cooperative supramolecular polymerization from macromolecular monomers. First, the macromolecular monomers should have multiple sites that allow strong intermolecular interactions to form the stable supramolecular polymers. Second, the interactions among the macromolecular monomers should be specific, directional, and cooperative,<sup>1a,2b</sup> as illustrated in Scheme 1. For these reasons, highly branched polymers<sup>5</sup> containing moieties that can be subject to multivalent H-bonding may be excellent macromolecular monomers for helical/tubular supramolecular polymerization. We recently reported the synthesis of comblike polynorbornene-*graft*-polypeptides (PN-*g*-PPs) via ring-opening metathesis polymerization (ROMP) of *N*-TMS-containing norbornenes followed by controlled ring-opening polymerization of amino acid *N*-carboxyanhydrides (ROP-NCAs) (Scheme 2).<sup>6</sup> Because the pendant polypeptides are excellent materials for H-bonding-directed assembly,<sup>5b,7</sup> we explored the possibility of utilizing PN-*g*-PP as the macromolecular monomer for supramolecular polymerization and subsequent molecular assembly (Scheme 1).

For tubular polymerization as illustrated in Scheme 1, the PN-*g*-PP macromolecular monomer should be soluble in the “polymerization” solution (e.g., water). Because poly(*L*-glutamic acid) (PLG) is highly water-soluble and can be readily prepared via ROP of *L*-glutamic acid NCA (Glu-NCA), we chose it as the PP to be grafted on PN. The PN-*g*-PLG synthesized and used in

**Received:** March 12, 2011

**Published:** July 15, 2011

**Scheme 2. Synthesis of PLG-Grafted Comblike Polymers (PN<sub>x</sub>-g-PLG<sub>n</sub>) by controlled ROMP and ROP-NCAs**


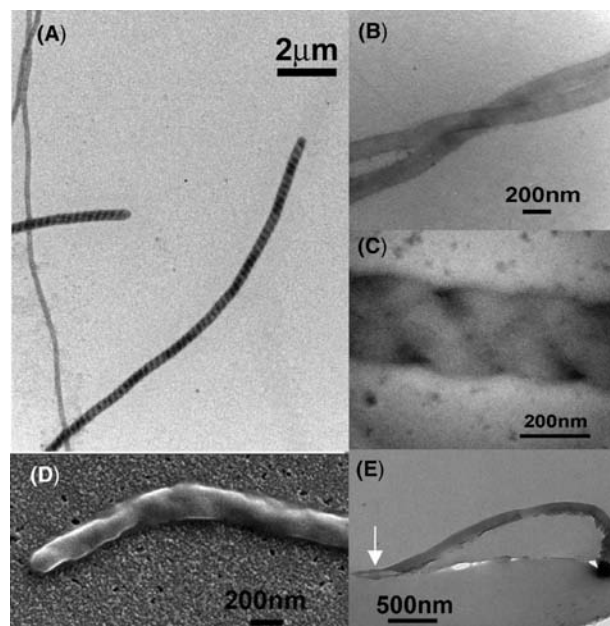
**Figure 1.** (A) Conformational changes in grafted PLGs at different pHs, as monitored by CD spectroscopy. The concentration of PN<sub>11</sub>-g-PLG<sub>101</sub> was 0.02 mg/mL. (B) TEM image of dispersed PN<sub>11</sub>-g-PLG<sub>101</sub> in a freshly made solution at pH 7 and 4 °C. The sample was stained with uranyl acetate. The inset shows DLS data for PN<sub>11</sub>-g-PLG<sub>101</sub> in the solution.

this study is denoted as PN<sub>x</sub>-g-PLG<sub>n</sub>, where *x* and *n* are the degrees of polymerization (DPs) of ROMP and Glu-NCA, respectively. PN<sub>11</sub>-g-PLG<sub>101</sub> with a short PN backbone (DP = 11) and a long PLG (DP = 101) was synthesized using the method we previously reported;<sup>6</sup> its structure and composition were confirmed by gel-permeation chromatography and <sup>1</sup>H NMR spectroscopy (Figures S1 and S2 and Table S1 in the Supporting Information).

As shown in the pH dependence of the molar ellipticity of PN<sub>11</sub>-g-PLG<sub>101</sub> at 222 nm (Figure 1A), PLG has protonated side chains at low pH, adopts a helical conformation, and becomes less water-soluble.<sup>8</sup> PN<sub>11</sub>-g-PLG<sub>101</sub> was found to form non-water-soluble aggregates rapidly at pH < 5 instead of forming ordered structures. At pH > 8, the side-chain carboxylate groups of the PLGs are ionized, and the PLGs thus adopt extended coil conformations as a result of charge repulsion.<sup>8</sup> The strong electrostatic repulsion between PN<sub>11</sub>-g-PLG<sub>101</sub> molecules at high pH also hinders their controlled assembly (i.e., the tubular polymerization of PN<sub>11</sub>-g-PLG<sub>101</sub> as illustrated in Scheme 1).

Appropriate pH is therefore critical for the controlled supramolecular polymerization of PN<sub>11</sub>-g-PLG<sub>101</sub>. Ideally, the PLG side chains should be partially protonated, allowing the PLGs to be water-soluble but reducing the charge repulsion in order to facilitate the intermolecular PLG-chain intercalation and subsequent formation of the antiparallel β-sheet conformation (see the PLG–PLG interaction illustrated in green in Scheme 1). The formation of antiparallel β-sheets is thermodynamically more favorable than parallel β-sheets or extended coils, which provides the required driving forces for the supramolecular polymerization.

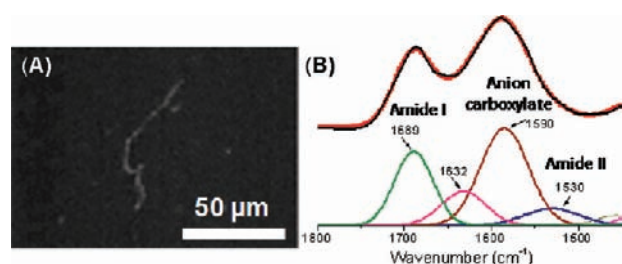
Thus, the pH for supramolecular polymerization of PN<sub>11</sub>-g-PLG<sub>101</sub> was selected from the middle point of the pH-induced helix–coil transition of grafted PLGs (Figure 1A). At pH 7 and reduced temperature (4 °C), PN<sub>11</sub>-g-PLG<sub>101</sub> was well-dispersed



**Figure 2.** (A–D) TEM and FESEM images of supramolecular structures assembled from (PN-g-PLG<sub>101</sub>)<sub>11</sub> in solution after incubation for 14 days at pH 7 and 4 °C. (E) TEM image of a supramolecular polymer embedded in epoxy resin and ultramicrotomed. The arrow indicates the edge of the supramolecular polymer as a result of microtome sectioning.

in its monomeric form initially, as evidenced by the transmission electron microscopy (TEM) and dynamic light scattering (DLS) analysis (Figure 1B), but started to form tubular supramolecular structures after a few days. Tubular polymerization of PN<sub>11</sub>-g-PLG<sub>101</sub> presumably starts with a slow nucleation step until an oligomer is formed with the first turn of the helix, as shown in Scheme 1. Subsequently, the number of interactions formed upon monomer addition increases, allowing for the cooperative growth of the supramolecular polymer.<sup>1a,2b</sup> The rate of the supramolecular polymerization depended on the initial concentration (*M*<sub>0</sub>) of PN<sub>11</sub>-g-PLG<sub>101</sub>, the monomer of supramolecular polymerization. Large tubular supramolecular structures appeared in solution within 7 days at pH 7 and 4 °C for *M*<sub>0</sub> = 30 μM. When *M*<sub>0</sub> was reduced to 3 μM, large supramolecular structures appeared after 60 days. After the formation of supramolecular structures, we found that the concentration of PN<sub>11</sub>-g-PLG<sub>101</sub> was reduced substantially (Figure S3).

Poly(PN<sub>11</sub>-g-PLG<sub>101</sub>), the supramolecular structures assembled from PN<sub>11</sub>-g-PLG<sub>101</sub>, were examined by electron microscopy and found to form very long tubular structures (Figure 2A–D). The typical poly(PN<sub>11</sub>-g-PLG<sub>101</sub>) with a length of 30 μm contains at least 10<sup>4</sup> PN<sub>11</sub>-g-PLG<sub>101</sub> repeating units, as estimated from the ratio of the effective volumes of the tubular structures and PN<sub>11</sub>-g-PLG<sub>101</sub>. The diameter of the tubular supramolecular structure was measured to be 170 ± 20 nm. The assertion of the supramolecular structure as tubules instead of solid rods or flat ribbons was based on the combination of TEM and field-emission scanning electron microscopy (FESEM) observations (Figure 2B,D). Solid cylindrical rods with such a large cross section would have shown prominent contrast between the center and the edge of the cylinders, which was not observed in our TEM experiments (Figure 2B). The FESEM image (Figure 2D) clearly shows the three-dimensional features expected from flexible tubular structures. For further characterization of the supramolecular structures, we removed

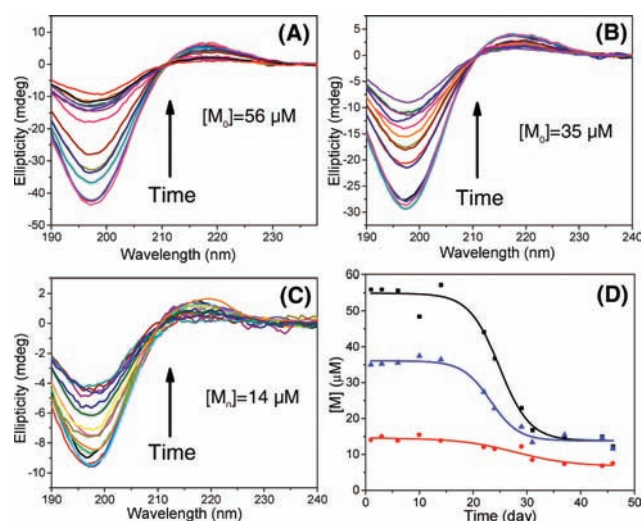


**Figure 3.** (A) Fluorescence microscopy image of a supramolecular polymer in solution after staining with ThT. (B) FTIR spectrum of poly(PN<sub>11</sub>-g-PLG<sub>101</sub>) and the assignment of the absorption peaks.

poly(PN<sub>11</sub>-g-PLG<sub>101</sub>) from the solution by centrifugation and embedded the supramolecular polymers in epoxy resin for microtoming. Under TEM, the edge of the poly(PN<sub>11</sub>-g-PLG<sub>101</sub>) from the microtome sectioning (indicated by the arrow in Figure 2E) revealed the characteristics of a hollow tube with a thin wall. Interestingly, some of the long, tubular supramolecular structures were further braided into superhelical structures, as evidenced by TEM analysis (Figure 2A), in particular at high magnification (Figure 2C).

While the grafted PLGs in PN<sub>11</sub>-g-PLG<sub>101</sub> had partially extended coil structures when dispersed in the pH 7 solution (Figure 1), their conformational structures changed upon assembly into the supramolecular polymers, adopting the anticipated antiparallel  $\beta$ -sheet conformation. The formation of  $\beta$ -sheet structures was confirmed via staining of poly(PN<sub>11</sub>-g-PLG<sub>101</sub>) with thioflavin T dye (ThT) (Figure 3A), a fluorescent molecule that is known for its strong, specific affinity to  $\beta$ -sheet structures.<sup>9</sup> The antiparallel nature of the  $\beta$ -sheet structures was revealed by FTIR analysis (Figure 3B and Figure S4), as the amide absorption peaks were consistent with the characteristic antiparallel  $\beta$ -sheet conformation on the basis of the assignment of the absorption peaks at 1689 cm<sup>-1</sup> (amide I), 1632 cm<sup>-1</sup> (amide I), and 1530 cm<sup>-1</sup> (amide II). The peak at 1590 cm<sup>-1</sup> was due to the ionized carboxylate groups.<sup>10</sup> The conclusion was further supported by wide-angle X-ray scattering (WAXS) analysis of an unoriented sample of poly(PN<sub>11</sub>-g-PLG<sub>101</sub>) (Figure S5A). The scattering pattern exhibited Bragg diffraction signals consistent with a semicrystalline polymer. The positions of the diffraction rings ( $q = 0.68, 0.97, \text{ and } 1.32 \text{ \AA}^{-1}$ ) correspond to the lattice spacing predicted for polypeptide chains arranged with a  $\beta$ -sheet conformation.<sup>11</sup> In comparison, the scattering pattern of a sample prepared by drying a freshly made PN<sub>11</sub>-g-PLG<sub>101</sub> solution showed only amorphous structures (Figure S5B). The structural change of the polypeptide-grafted comb polymers during the assembly process is in excellent agreement with the proposed supramolecular polymerization mechanism illustrated in Scheme 1.

We then examine whether the supramolecular polymerization is a cooperative process. Cooperativity due to the formation of tubular supramolecular polymers can arise from the unique disposition of repeating units in the tubular structures, as each unit is simultaneously in contact with multiple neighbors after formation of the first helical turn (Scheme 1). Accordingly, the initial polymerization is thermodynamically less favorable than propagation, which results in a time-dependent lag in the growth of the polymers (nucleation step).<sup>2b</sup> The kinetic process of the supramolecular polymerization was studied by monitoring the concentration change of a PN<sub>10</sub>-g-PLG<sub>95</sub> polymer in solution with time using circular dichroism (CD) spectroscopy (Figure 4). Three polymer solutions ( $M_0 = 56, 35, \text{ and } 14 \mu\text{M}$ ) were first

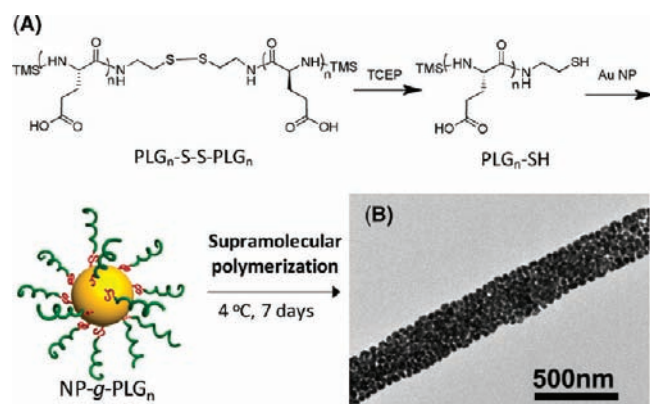


**Figure 4.** Kinetic study of the supramolecular polymerization from PN<sub>10</sub>-g-PLG<sub>95</sub> at pH 7 and 4 °C. (A–C) Change in ellipticity of the supernatant with time, as monitored by CD spectroscopy. For each measurement, 50  $\mu\text{L}$  solutions were removed from individual stock solutions and centrifuged at 10 000 rpm at 4 °C for 20 min to remove the supramolecular polymers. The supernatants were then diluted 20 $\times$  for CD spectroscopy. (D) Supramolecular polymerization kinetics of PN<sub>10</sub>-g-PLG<sub>95</sub>, starting from initial polymer concentrations of 56  $\mu\text{M}$  (black), 35  $\mu\text{M}$  (blue) and 14  $\mu\text{M}$  (red).

filtered to remove dust and other impurities in order to avoid nucleation on a foreign substrate, after which they were incubated at 4 °C without stirring. The formation of supramolecular polymers depleted the freely dispersed PN<sub>10</sub>-g-PLG<sub>95</sub> in solution, corresponding to the decrease in the ellipticity of the supernatants (Figure 4A–C). As shown in Figure 4D, the growth of the supramolecular polymers occurred in two distinct stages, with a slow nucleation step followed by faster chain propagation. The rate of polymerization depended moderately on the concentration, suggesting a large critical nucleus size. The sigmoidal transitions found in all of the kinetic experiments indicate a highly cooperative process in the supramolecular polymerization.<sup>2b</sup> Much higher polymerization rates were found for solutions containing a small amount of polymerization “seeds” (data not shown). A complete kinetic analysis is the subject of future studies, which may elucidate the exact molecular mechanism of the cooperative supramolecular polymerization from these comb polymers.

We next prepared a few other comblike polymers with different lengths of PN or PLG (PN<sub>11</sub>-g-PLG<sub>62</sub> and PN<sub>18</sub>-g-PLG<sub>128</sub>) and demonstrated the general applicability of the supramolecular polymerization (Tables S1 and S2 and Figure S6). The external diameters of the tubular structures were found to correlate with the size of macromolecular monomers, with values of  $70 \pm 10 \text{ nm}$  for PN<sub>11</sub>-g-PLG<sub>62</sub> and  $420 \pm 50 \text{ nm}$  for PN<sub>18</sub>-g-PLG<sub>128</sub> (Figure S6). It is unclear how the diameter of the poly(PN-g-PLG) correlates with the lengths of PN and PLG, but apparently, both parameters substantially affect the packing of PN-g-PLG in the supramolecular structures. We also found that the multivalent nature of the comblike polymers is crucial for the cooperative supramolecular polymerization; no supramolecular polymerization was observed with diblock PLG with a disulfide linker [(PLG<sub>97</sub>)<sub>2</sub>] or a Y-shaped PLG [(PLG<sub>94</sub>)<sub>3</sub>] (Scheme S1 and Tables S1 and S2), although their PLG chain lengths were similar to that in PN<sub>11</sub>-g-PLG<sub>101</sub>.





**Figure 5.** (A) Synthesis of PLG-grafted gold NPs (NP-g-PLG<sub>n</sub>). (B) TEM image of tubular supramolecular structures assembled from NP-g-PLG<sub>55</sub> in pH 7 solution after incubation for 7 days at 4 °C.

PN-g-PLG at pH 7 has partially charged PLG side chains that are likely spherically extended in space because of intramolecular PLG–PLG repulsion. The supramolecular polymerization of PN-g-PLG appears to be dictated by the intermolecular PLG–PLG antiparallel  $\beta$ -sheet formation, and PN is unlikely to provide any critical molecular interaction force for the polymerization. It is reasonable to believe that the backbone of the monomer does not have to be a polymer for the controlled tubular supramolecular polymerization to occur, and any globular nanoparticles (NPs) with surface-grafted PLGs should also be subject to controlled polymerization. To test this hypothesis, we synthesized gold NPs with surface-grafted PLGs (NP-g-PLG) (Figure 5A; also see the Supporting Information) and performed the supramolecular polymerization experiments under condition similar to those for PN-g-PLG. Our study demonstrated that NP-g-PLG can undergo a similar polymerization process to form tubular supramolecular structures [poly(NP-g-PLG)] (Figure 5B) that is facilitated by inter-NP PLG-chain intercalation and subsequent formation of an antiparallel  $\beta$ -sheet conformation.

In conclusion, by controlling the interactions of polypeptide-grafted comblike polymers, we achieved supramolecular polymerization of these large macromolecular monomers under specific solution conditions. The resulting tubular supramolecular structures have external diameters of hundreds of nanometers and lengths of up to 50  $\mu$ m. The tubular supramolecular structure could withstand extensive centrifugation and be isolated from the solution and was remarkably stable (it could be stored at room temperature for more than 6 months). Therefore, this supramolecular polymerization process allows us to access tubular poly(macromolecules) and poly(nanoparticles) as a new class of materials with their collective properties and applications to be explored. Further investigation may pave the way to the development of artificial systems that may approach the level of sophistication and complexity found in nature's self-organized, supramolecular polymers with desired material properties.<sup>12</sup>

## ■ ASSOCIATED CONTENT

**Supporting Information.** Experimental procedures and characterization of the polymers and the supramolecular structures. This material is available free of charge via the Internet at <http://pubs.acs.org>.

## ■ AUTHOR INFORMATION

### Corresponding Author

ylin@ims.uconn.edu; jianjunc@illinois.edu.

## ■ ACKNOWLEDGMENT

Y.L. acknowledges support from the Faculty Startup Fund and the Research Foundation at the University of Connecticut. J.C. acknowledges support from NSF (CHE-0809420). V.U. acknowledges support from DOE BES. We thank Prof. C. Vijaya Kumar for helpful inputs to this research.

## ■ REFERENCES

- (1) (a) Oosawa, F.; Kasai, M. *J. Mol. Biol.* **1962**, *4*, 10. (b) Sept, D.; McCammon, J. A. *Biophys. J.* **2001**, *81*, 667. (c) Yeates, T. O.; Padilla, J. E. *Curr. Opin. Struct. Biol.* **2002**, *12*, 464.
- (2) (a) Brunsveld, L.; Folmer, B. J. B.; Meijer, E. W.; Sijbesma, R. P. *Chem. Rev.* **2001**, *101*, 4071. (b) De Greef, T. F. A.; Smulders, M. M. J.; Wolfs, M.; Schenning, A. P. H. J.; Sijbesma, R. P.; Meijer, E. W. *Chem. Rev.* **2009**, *109*, 5687. (c) Yan, D.; Zhou, Y.; Hou, J. *Science* **2004**, *303*, 65. (d) Whitesides, G. M.; Grzybowski, B. *Science* **2002**, *295*, 2418.
- (3) (a) Iwaura, R.; Hoeben, F. J. M.; Masuda, M.; Schenning, A. P. H. J.; Meijer, E. W.; Shimizu, T. *J. Am. Chem. Soc.* **2006**, *128*, 13298. (b) Fox, J. D.; Rowan, S. J. *Macromolecules* **2009**, *42*, 6823. (c) Koga, T.; Taguchi, K.; Kobuke, Y.; Kinoshita, T.; Higuchi, M. *Chem.—Eur. J.* **2003**, *9*, 1146. (d) García, F.; Aparicio, F.; Marenchino, M.; Campos-Olivas, R.; Sánchez, L. *Org. Lett.* **2010**, *12*, 4264. (e) Li, L. S.; Jiang, H. Z.; Messmore, B. W.; Bull, S. R.; Stupp, S. I. *Angew. Chem., Int. Ed.* **2007**, *46*, 5873.
- (4) (a) Cornelissen, J. J. L. M.; Fischer, M.; Sommerdijk, N. A. J. M.; Nolte, R. J. M. *Science* **1998**, *280*, 1427. (b) Stupp, S. I.; LeBonheur, V.; Walker, K.; Li, L. S.; Huggins, K. E.; Keser, M.; Amstutz, A. *Science* **1997**, *276*, 384. (c) Cui, H. G.; Chen, Z. Y.; Zhong, S.; Wooley, K. L.; Pochan, D. J. *Science* **2007**, *317*, 647. (d) Percec, V.; Ahn, C. H.; Ungar, G.; Yeardley, D. J. P.; Moller, M.; Sheiko, S. S. *Nature* **1998**, *391*, 161. (e) Murnen, H. K.; Rosales, A. M.; Jaworski, J. N.; Segalman, R. A.; Zuckermann, R. N. *J. Am. Chem. Soc.* **2010**, *132*, 16112.
- (5) (a) Gitsas, A.; Floudas, G.; Mondeshki, M.; Butt, H. J.; Spiess, H. W.; Iatrou, H.; Hadjichristidis, N. *Biomacromolecules* **2008**, *9*, 1959. (b) Klok, H. A.; Rodriguez-Hernandez, J. *Macromolecules* **2002**, *35*, 8718. (c) Sheiko, S. S.; Sumerlin, B. S.; Matyjaszewski, K. *Prog. Polym. Sci.* **2008**, *33*, 759.
- (6) Lu, H.; Wang, J.; Lin, Y.; Cheng, J. J. *J. Am. Chem. Soc.* **2009**, *131*, 13582.
- (7) (a) Breitenkamp, R. B.; Ou, Z.; Breitenkamp, K.; Muthukumar, M.; Emrick, T. *Macromolecules* **2007**, *40*, 7617. (b) Mondeshki, M.; Mihov, G.; Graf, R.; Spiess, H. W.; Mullen, K.; Papadopoulos, P.; Gitsas, A.; Floudas, G. *Macromolecules* **2006**, *39*, 9605. (c) Percec, V.; Dulcey, A. E.; Balagurusamy, V. S. K.; Miura, Y.; Smidrkal, J.; Peterca, M.; Nummelin, S.; Edlund, U.; Hudson, S. D.; Heiney, P. A.; Hu, D. A.; Magonov, S. N.; Vinogradov, S. A. *Nature* **2004**, *430*, 764.
- (8) (a) Nagasawa, M.; Holtzer, A. *J. Am. Chem. Soc.* **1964**, *86*, 538. (b) O'Neil, K. T.; DeGrado, W. F. *Science* **1990**, *250*, 646. (c) Spek, E. J.; Gong, Y.; Kallenbach, N. R. *J. Am. Chem. Soc.* **1995**, *117*, 10773. (d) Tiffany, M. L.; Krimm, S. *Biopolymers* **1972**, *11*, 2309.
- (9) (a) Levine, H. *Protein Sci.* **1993**, *2*, 404. (b) LeVine, H., III. *Methods Enzymol.* **1999**, *309*, 274.
- (10) (a) Lee, N. H.; Frank, C. W. *Langmuir* **2003**, *19*, 1295. (b) Shim, J. Y.; Gupta, V. K. *J. Colloid Interface Sci.* **2007**, *316*, 977.
- (11) (a) Fändrich, M.; Dobson, C. M. *EMBO J.* **2002**, *21*, 5682. (b) Keith, H. D.; Giannoni, G.; Padden, F. J. *Biopolymers* **1969**, *7*, 775.
- (12) (a) Smith, J. F.; Knowles, T. P. J.; Dobson, C. M.; MacPhee, C. E.; Welland, M. E. *Proc. Natl. Acad. Sci. U.S.A.* **2006**, *103*, 15806. (b) Lee, C. C.; Nayak, A.; Sethuraman, A.; Belfort, G.; McRae, G. J. *Biophys. J.* **2007**, *92*, 3448.